

Phenothiazine-Sensitized Organic Solar Cells: Effect of Dye Anchor Group Positioning on the Cell Performance

Aaron S. Hart,[†] Chandra Bikram K. C.,[†] Navaneetha K. Subbaiyan,[†] Paul A. Karr,[‡] and Francis D'Souza^{*†}

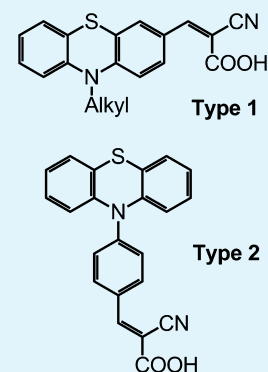
[†]Department of Chemistry, University of North Texas, 1155 Union Circle, #305070, Denton, Texas 76203-5017, United States

[‡]Department of Physical Sciences and Mathematics, Wayne State College, 111 Main Street, Wayne, Nebraska 68787, United States

S Supporting Information

ABSTRACT: Effect of positioning of the cyanoacrylic acid anchoring group on ring periphery of phenothiazine dye on the performance of dye-sensitized solar cells (DSSCs) is reported. Two types of dyes, one having substitution on the C-3 aromatic ring (Type 1) and another through the N-terminal (Type 2), have been synthesized for this purpose. Absorption and fluorescence studies have been performed to visualize the effect of substitution pattern on the spectral coverage and electrochemical studies to monitor the tuning of redox levels. B3LYP/6-31G* studies are performed to visualize the frontier orbital location and their significance in charge injection when surface modified on semiconducting TiO₂. New DSSCs have been built on nanocrystalline TiO₂ according to traditional two-electrode Grätzel solar cell setup with a reference cell based on N719 dye for comparison. The lifetime of the adsorbed phenothiazine dye is found to be quenched significantly upon immobilizing on TiO₂ suggesting charge injection from excited dye to semiconducting TiO₂. The performances of the cells are found to be prominent for solar cells made out of Type 1 dyes compared to Type 2 dyes. This trend has been rationalized on the basis of spectral, electrochemical, computational, and electrochemical impedance spectroscopy results.

KEYWORDS: photovoltaic, phenothiazine, organic solar cell, impedance spectroscopy, light energy conversion



1. INTRODUCTION

Dye-sensitized solar cells (DSSCs) have attracted significant attention as potential low-cost replacements to silicon-based photovoltaic technology.¹ High-performance sensitizers capable of wide-band spectral capture are recognized to be a promising strategy for improving the cost-efficiency of the DSSCs. In this regard, organic photosensitizers are recognized to be ideal replacements for traditionally used, relatively expensive, ruthenium metal complex based sensitizers. The metal free organic dyes have much stronger light-harvesting ability than metal complexes because of their high molar extinction coefficients. The common solar dye-design involves donor connected to an electron acceptor anchoring functionality which allows fine-tuning of optical and electrochemical properties. For donors, dialkylaminophenyl groups,^{8–10} coumarins,¹¹ triphenylamines,^{12–14} indoline,^{15,16} phenothiazine,^{17–20} polythiophene,²¹ porphyrin,^{22–28} phthalocyanine,²⁹ and quantum dots^{30–32} have been successfully utilized. The choice of electron acceptor anchoring functionality in the design is largely based on cyanoacrylic acid functionality although other electron acceptors such as fullerenes,^{24–26} nanotubes,^{33,34} and other two-dimensional electron acceptors³⁵ are being developed and optimized by several research groups. The cyanoacrylic acid functionality largely fulfills the need of an electron acceptor while providing the carboxylic acid group to bind nanocrystalline semiconductor surface.

For efficient design of donor-spacer-acceptor dyes, one of the key issues relates to the positioning of the electron acceptor anchoring group on the macrocycle periphery. The dye-

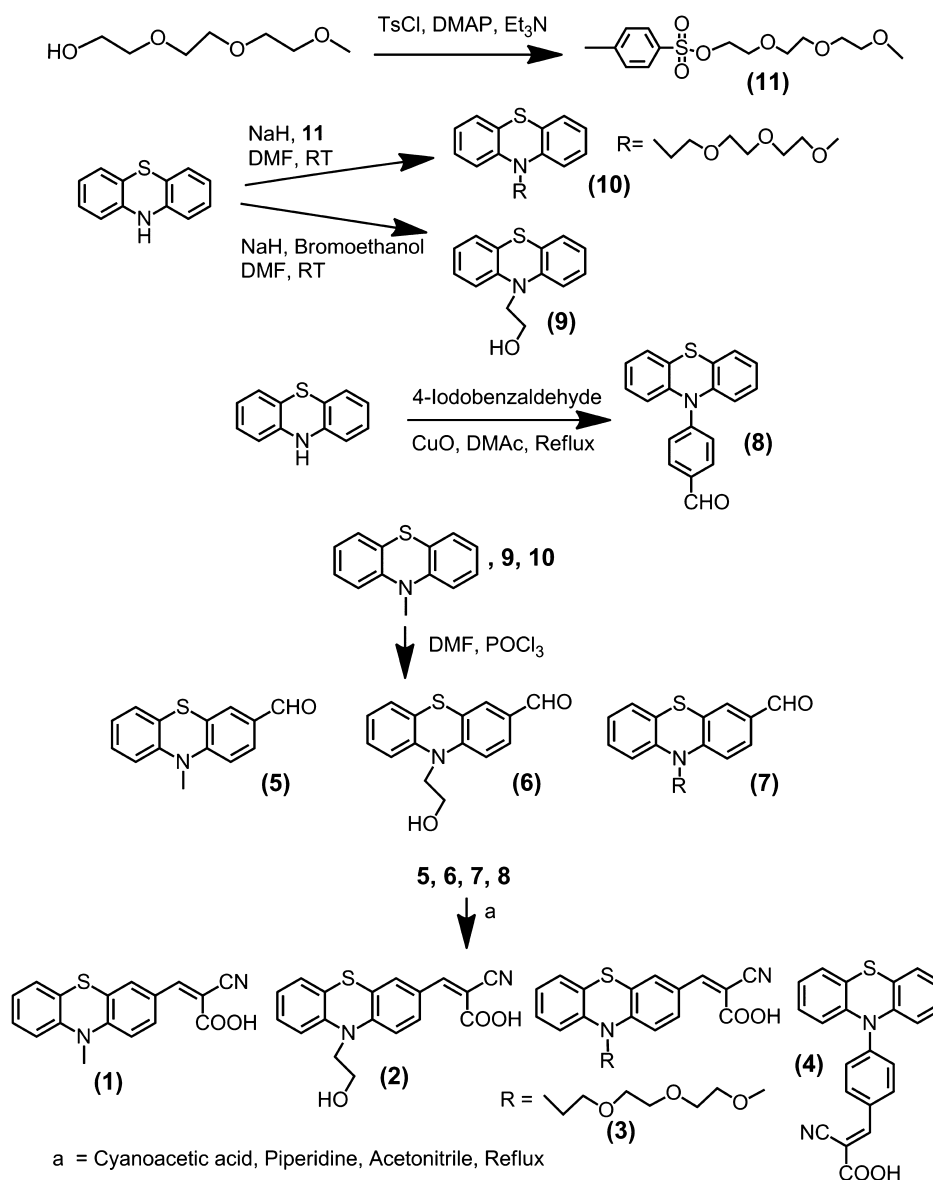
nanoparticle interaction which depends upon the orientation and positioning of the HOMO-LUMO orbitals for efficient charge injection can be fine-tuned by proper dye-nanoparticle immobilization. For example, in case of porphyrin-TiO₂ solar cells, the positioning of carboxy group on the *meso*-phenyl groups is shown to vary the performance of the solar cell.³⁶ However, such studies on other high performance dyes are scarce, perhaps due to associated synthetic challenges. In the present study, we have undertaken such a task on a well-known for photoelectrochemical applications, phenothiazine dye,^{37–40} and report on the effect of positioning of the cyanoacrylic acid functionality on the dye molecule. For this, we have synthesized two types of dyes, viz., dyes having the substitution at the aromatic ring carbon (Type 1, compounds 1-3 in Scheme 1) and a dye with substitution through the hetero N-atom of the macrocycle (Type 2, compound 4 in Scheme 1). The phenothiazine dyes contain electron-rich sulfur and nitrogen atoms, have non-planar geometry, and exhibit good thermal and electrochemical stability. For Type 1 dyes, the N-atom of the phenothiazine ring was substituted with a methyl, 2-hydroxyethane, or tris(ethyleneglycol) methyl ether groups to visualize their effect, primarily, on preventing aggregation. Additionally, theoretical calculations using DFT methods have been performed in order to optimize the geometry and to visualize location of the HOMOs and LUMOs. The dyes are

Received: July 24, 2012

Accepted: October 8, 2012

Published: October 8, 2012

Scheme 1. Synthetic Route Adapted for the Preparation of Cyanoacrylic Acid Functionalized Phenothiazine Dyes for Solar Cell Construction



then used as sensitizers in DSSCs fabrication, and the device performance is evaluated. The better performance of the cells observed for Type 1 dyes is rationalized from electrochemical impedance spectroscopy measurements (EIS) among other techniques.

2. RESULTS AND DISCUSSION

Syntheses of Cyanoacrylic Acid Functionalized Phenothiazine Dyes. The methodology developed for the synthesis of cyanoacrylic acid functionalized at different positions of phenothiazine is shown in Scheme 1 while the details are given in the Experimental Section. Briefly, tri(ethylene glycol)monomethyl ether tosylate (**11**) was synthesized by the reaction of tri(ethylene glycol)monomethyl ether with *p*-toluene sulfonyl chloride. The 10-(2-hydroxyethane)phenothiazine (**9**) was synthesized by reacting phenothiazine with 2-bromoethanol in DMF in the presence of NaH . Similarly, 10-(triethyleneglycol monomethyl ether) phenothiazine (**10**) was synthesized by reacting phenothiazine and **11** in

DMF in the presence of NaH . Next, *N*-methyl phenothiazine, **10** and **11** were formylated to their respective carboxaldehyde derivatives, (**5**, **6** and **7**) by standard Vilsmeier formylation procedure by the reaction of the respective compounds with POCl_3 in DMF at low temperature. The 10-(4-formylphenyl) phenothiazine (**8**) was synthesized by reacting phenothiazine with 4-iodobenzaldehyde and CuO in *N,N*-dimethylacetamide (DMAc) as solvent. Finally, the electron acceptor anchoring group, cyanoacrylic acid was introduced by reacting respective phenothiazine aldehyde derivatives (**5**, **6**, **7**, or **8**) with cyanoacetic acid in the presence of piperidine as catalyst in acetonitrile, to obtain compounds **1–4**, respectively. The newly synthesized dyes have been fully characterized by mass, ^1H NMR, and other spectroscopic techniques.

Optical Absorption and Steady-State Fluorescence Studies. Figure 1a shows the absorption spectra of the investigated compounds along with pristine phenothiazine used as a control. Phenothiazine revealed a peak at 318 nm in *o*-dichlorobenzene (DCB). Introducing the cyanoacrylic acid

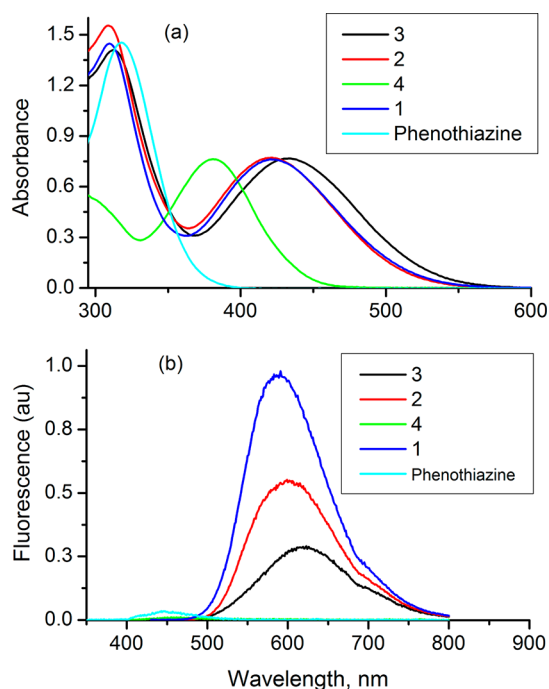


Figure 1. (a) Absorption (normalized to the visible band position) and (b) fluorescence emission spectrum of the indicated compounds in DCB at RT. The compounds were excited at the respective visible peak maxima.

functionality revealed drastic spectral changes. That is, for compound 4 with cyanoacrylic acid functionality at the N atom, this band was red shifted to 381 nm. Interestingly, for compounds 1–3 having substitution at the aromatic carbon, the spectra revealed a split band, the first UV band in the 308–312 nm range and a visible band in the 420–433 nm range. Earlier, the shorter wavelength band was assigned to the localized aromatic π – π^* transition of the phenothiazine ring and the long wavelength one to the charge-transfer (CT) transition.³⁷ The intensity of the π – π^* was higher than that of the CT transition. The key observation is the spectral coverage for the two types of phenothiazine derivatives. Type 1 derivatives revealed spectral coverage from UV until about 550 nm while for the Type 2 dye, the spectral coverage was only until 450 nm. It is known that broad optical coverage is favorable for the performance of DSSCs, as more photons could be harvested.⁴¹ Using the molar extinction coefficient of each visible band, estimated dye concentrations were found to be 0.070, 0.085, 0.149, and 0.041 mM, for 1, 2, 3, and 4, respectively.

Figure 1b shows the emission spectrum of the investigated compounds for concentrations normalized to the visible band intensity (Figure 1a) in DCB. The Type 1 phenothiazine derivatives revealed a broad emission in the range of 580–620 nm. The relative emission quantum yield was found to depend upon the type of substituent on the N-atom being 1 (methyl) > 2 (2-hydroxyethane) > 3 (triethylene glycol monomethyl ether). Interestingly, Type 2 compound, 4, and the control phenothiazine had a small emission peak around 450 nm (<2% intensity compared to Type 1 compounds). The better spectral coverage and emission properties covering most of the visible portion of the spectrum of Type 1 derivatives suggest them being better DSSC dyes compared to Type 2 dye.

Computational and Electrochemical Studies. Molecular orbital calculations using B3LYP/6-31G* basis set⁴² were performed to arrive at the geometry and electronic structure of Type 1 and Type 2 compounds. The structures were fully optimized on Born-Oppenheimer potential energy surface, and the frequency calculations revealed absence of negative frequencies. Figure 2a and 2d show the optimized structures

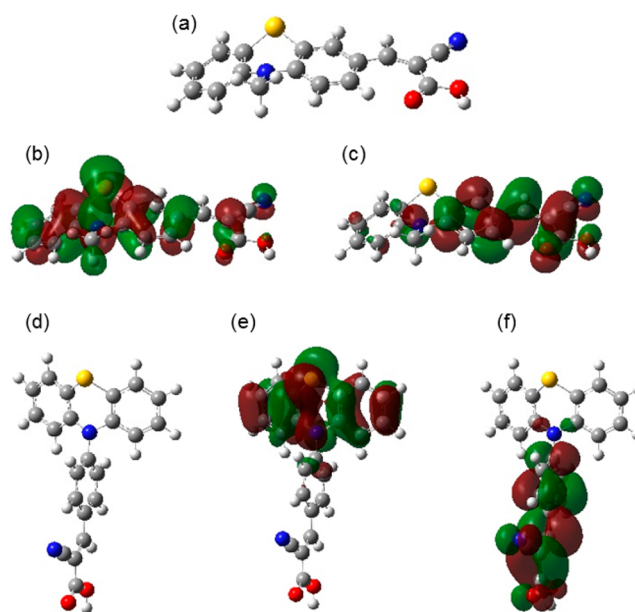


Figure 2. (a, d) B3LYP/6-31G* optimized structures, and frontier (b, e) HOMO and (c, f) LUMO of compounds (a–c) 1 and (d–f) 4.

of 1 and 4 representing Type 1 and Type 2 compounds, respectively. The non-planar structure of phenothiazine macrocycles was clear for both types of compounds which would result in reduced dye-aggregation. That is, the angle between two terminal phenyl rings was 149° from the sulfur side, and 144° from the nitrogen side of the macrocycle. The cyanoacrylic acid functionality was in-plane with the substituted phenyl ring of phenothiazine in case of 1 while for 4, the phenyl cyanoacrylic acid functionality was perpendicular the phenothiazine ring. The frontier HOMO was found to be largely located on the phenothiazine macrocycle (Figures 2b and e) while the LUMO was on the cyanoacrylic acid group and part of the macrocycle in case of 1 (Figure 1c) while for 4 it was fully on the phenyl cyanoacrylic acid functionality (Figure 1f). The location of the LUMOs favors electron injection from excited phenothiazine to the semiconductor conduction band when bound to the TiO_2 surface.

Further, electrochemical studies using differential pulse voltammetry were performed to evaluate the oxidation potential of the phenothiazine dyes and to estimate the energetics of electron transfer from excited dye to the conduction band of TiO_2 . The first oxidation process of pristine phenothiazine was found to be located at 0.61 V vs. Fc/Fc^+ in DCB containing 0.1 M TBAClO_4 . Substitution of cyanoacrylic acid functionality made the ring oxidation harder, more so for the Type 1 dyes compared to Type 2 dye. That is, an anodic shift of over 280 mV for Type 1 dyes (0.98 V for 2, 0.89 V for 1 and 3 vs. Fc/Fc^+) and 110 mV for Type 2 dye (0.71 V vs. Fc/Fc^+ for 4) was observed (see Figure S1 in the Supporting Information for DPVs). The easier oxidation of N-

substituted with electron acceptor anchoring group of compound **4** was noteworthy from this study.

The energetics for electron injection were estimated from electrochemical and emission data. The singlet excited state energy, $E_{0,0}$ for the phenothiazine dyes were calculated from the optical absorption and emission data and were found to be 2.43–2.50 eV for Type 1 dyes and 2.97 eV for Type 2 dye. By converting the oxidation potential to SHE (1.26 V for Type 1 and 1.11 eV for Type 2 dyes) the excited state potential corresponding to the LUMO level ($= E_{ox} - E_{0,0}$) were estimated. These values were found to range between -1.17 and -1.24 V for Type 1 and -1.85 V for Type 2 dyes. The sufficiently negative LUMO levels of these dyes compared to the conduction band energy of TiO_2 being -0.5 V vs. SHE implies possibility of electron injection from the excited dye into the conduction band of TiO_2 . Additionally, the HOMO levels of the investigated dyes are sufficiently more positive than the iodine/iodide redox couple value being 0.40 V. This indicates the oxidized dyes formed after electron injection into the conduction bands of TiO_2 could thermodynamically accept electron from the iodide ions.

The fluorescence lifetimes of the investigated compounds were studied both in acetonitrile and modified on TiO_2 surface. Phenothiazine and the studied compounds revealed a monoexponential decay with lifetimes of 0.99, 5.02, 5.41, 5.9, and 0.55 ns, respectively, for phenothiazine, **1**, **2**, **3**, and **4** (see Figure S2 in the Supporting Information). Next, these compounds were adsorbed on quartz slide modified with thin-layer of TiO_2 . Significant quenching was observed indicating occurrence of excited state events from the singlet excited phenothiazine to TiO_2 . The average lifetime of compound **1** on TiO_2 surface was found to be 0.21 ns, however, for other compounds on TiO_2 surface, the lifetimes were smaller than 0.2 ns, less than the detection limit of the lifetime measurement setup used in the present study.

Photoelectrochemical Studies. Figure 3 shows the current–voltage characteristics of dye-sensitized solar cells employing both Type 1 and Type 2 phenothiazine dyes as sensitizers under standard global AM1.5 solar light conditions. Sandwich type two-electrode cells were built using dye-coated TiO_2 film as working electrode, platinized FTO as the counter

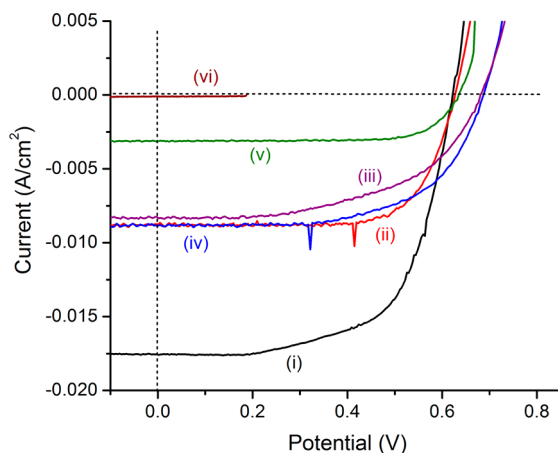


Figure 3. Photocurrent density vs. voltage (I - V) curves of DSSCs built using (i) N719, (ii) **3**, (iii) **1**, (iv) **2**, and (v) **4** dyes as sensitizers under irradiation of AM 1.5 simulated solar light (100 mW cm^{-2}) in the presence of I^-/I_3^- redox mediator in acetonitrile. The curve (vi) shows I - V behavior of FTO/ TiO_2 in the absence of any adsorbed dye.

electrode, I^-/I_3^- as redox mediator in the presence of 4-*tert*-butylpyridine in acetonitrile. The losses of light reflection and absorption by the conducting glass were not corrected. The amount of dye adsorbed was estimated by desorbing the dye using NaOH and from known molar extinction coefficient of phenothiazine. Such analysis provided ~ 2.2 – $5.0 \times 10^{-7} \text{ mol/cm}^2$ for Type 1 and $\sim 1.8 \times 10^{-7} \text{ mol/cm}^2$ for Type 2 dyes, being close in surface coverage of the dyes. A steady anodic photocurrent was observed when the electrodes were illuminated, and reproducible photocurrents were observed during on-off photo-switching revealing the robustness of the dye material developed here. The photovoltaic characteristic parameters of short-circuit currents density (I_{sc}), open-circuit potential (V_{oc}), fill factor (FF), and photovoltaic conversion efficiency (η) are given in Table 1 along with a DSSC built

Table 1. Photovoltaic Performance of DSSCs Based on Type 1 and Type 2 Phenothiazine Dyes with Liquid Electrolyte

dye	J_{sc} (mA/cm^2)	V_{oc} (V)	FF	η (%)	amount (mol/cm^2)
N719	18.13	0.62	0.66	7.39	
1	6.50	0.66	0.75	3.21	2.18×10^{-7}
2	8.03	0.65	0.75	3.88	4.09×10^{-7}
3	8.36	0.66	0.74	4.07	5.02×10^{-7}
4	2.75	0.62	0.77	1.30	1.82×10^{-7}

using N719 sensitizer for comparison. As shown in Table 1, photovoltaic conversion efficiencies for Type 1 dyes were higher compared to Type 2 dye. The highest η of 4.07% was obtained for compound **3** having aggregation preventing ethylene glycol substituent at the N-atom. On the contrary compound **4**, a Type 2 dye bearing phenyl cyanoacrylic acid functionality revealed the lowest conversion efficiency of 1.3% even though this compound was easier to oxidize by $\sim 150 \text{ mV}$ compared to the other studied Type 1 dyes. It is also interesting to note that although the V_{oc} were almost the same for all of the cells including that of N719 cell, the fill factors for the phenothiazine dyes were much better than that for the N719 dye based DSSC.

The monochromatic incident photon-to-current conversion efficiency (IPCE), defined as the number of electrons generated by light in the outer circuit divided by the number of incident photons, was determined according to eq 1⁴³

$$\text{IPCE (\%)} = 100 \times 1240 \times I_{SC} (\text{mA cm}^{-2}) / [\lambda (\text{nm}) \times P_{in} (\text{mW cm}^{-2})] \quad (1)$$

where I_{SC} is the short-circuit photocurrent generated by the incident monochromatic light and λ is the wavelength of this light with intensity P_{in} . The photocurrent action spectrum of the FTO/ TiO_2 modified electrodes with listed dyes in Table 1 is shown in Figure 4. The Type 1 dyes efficiently converted visible light to photocurrent in the region from 400–625 nm, whereas the Type 2 dye covered a shorter range being 400–510 nm. It is important to note that the IPCE spectrum revealed red-shifted bands compared to absorption spectral peaks shown in Figure 1a. However, these spectral features were similar to the spectrum of the respective phenothiazine derivatives adsorbed on FTO/ TiO_2 surface (see Figure S3 in the Supporting Information), suggesting such red shift could be due to dye aggregation on the electrode surface. The IPCE exceeded 70% at the peak maxima, however lower in terms of

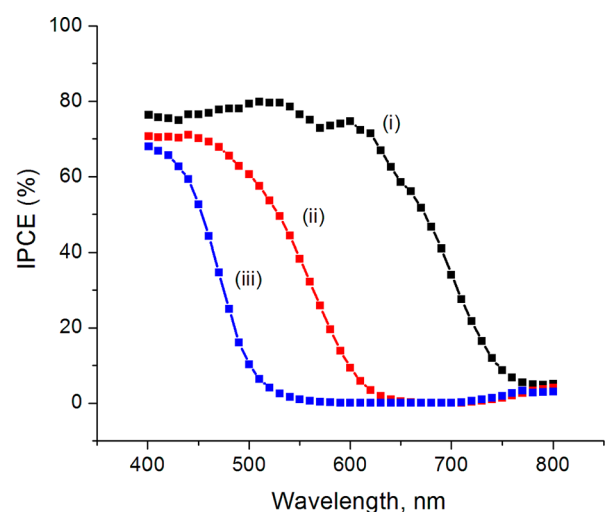


Figure 4. (a) Incident photon-to-current conversion action spectra of TiO_2 electrodes sensitized with (i) N719, (ii) 3, and (iii) 4 dyes in acetonitrile containing I_3^-/I^- (0.6 M PMII, 0.1 M LiI 0.05 M I_2 , and 0.5 M TBP) redox mediator using an AM 1.5 simulated light source with a 350 nm UV-cut off filter.

spectral coverage and efficiency when compared to N719 dye-based DSSC.

Electrochemical Impedance Spectroscopy Studies. To further understand the $\text{FTO}/\text{TiO}_2/\text{dye}$ interface, we performed electrochemical impedance spectroscopy studies (EIS) since this technique has been a useful tool to estimate electron recombination resistance and to know the dye regeneration efficiency.⁴³ Figure 5 shows EIS results for DSSCs comprised of $\text{FTO}/\text{TiO}_2/3$ and $\text{FTO}/\text{TiO}_2/4$ electrodes, representative of Type 1 and Type 2 type dyes, under illuminated and dark

conditions covering a frequency range of 100 kHz to 50 mHz. Significant differences between Type 1 and Type 2 dye-sensitized solar cells were found for the conductivity. The Nyquist plots (Figure 5) showed the radius of the semicircle corresponding to the working electrode to be higher for $\text{FTO}/\text{TiO}_2/4$ compared to $\text{FTO}/\text{TiO}_2/3$ indicating that the electron recombination resistance increases for 4 to 3 dye modified electrodes. The recombination resistance (R_{CT}) under dark conditions for $\text{FTO}/\text{TiO}_2/3$ and $\text{FTO}/\text{TiO}_2/4$ were 10.4 and 43.3 Ωcm^2 , respectively, whereas these values under AM1.5 light conditions at V_{oc} were 8.0 and 36.6 Ωcm^2 , respectively (see Table 2 for data on other Type 1 dyes). Clearly higher R_{CT}

Table 2. Recombination Resistance for $\text{FTO}/\text{TiO}_2/\text{Dye}$ Modified Electrodes Estimated from Electrochemical Impedance Spectroscopy Method

dye	condition	R_{CT} (Ωcm^2)
1	dark	27.6
	light	17.8
2	dark	10.0
	light	6.9
3	dark	10.4
	light	8.0
4	dark	43.3
	light	36.6

was obtained for Type 2 dyes under dark and light conditions indicating poor electron injection. The decrease in recombination resistance for $\text{FTO}/\text{TiO}_2/3$ compared to $\text{FTO}/\text{TiO}_2/4$ under light condition can be attributed to the better performance, i.e., photo-regeneration of $\text{FTO}/\text{TiO}_2/3$ is much efficient in the former case, a result that agrees well

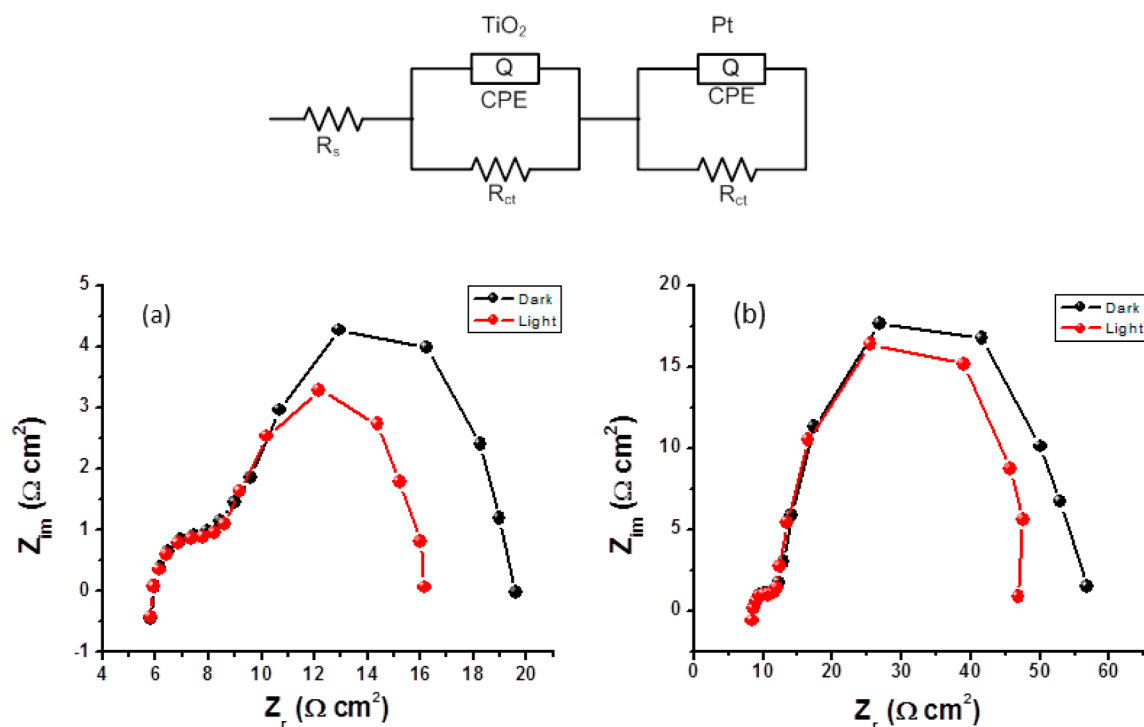


Figure 5. Impedance spectra (Nyquist plots) measured at the respective open circuit potential (V_{OC}) of (a) $\text{FTO}/\text{TiO}_2/3$ and (b) $\text{FTO}/\text{TiO}_2/4$ in dark (dark lines) and under AM1.5 light conditions (red lines), respectively. The figure top panel shows equivalent circuit diagram used to fit the experimental data.

with the cell efficiency shown in Figures 3 and 4. Under similar conditions, N719 dye was tested and found to be in good agreement with the literature results.⁴²

3. SUMMARY

In summary, four phenothiazine dyes functionalized with a cyanoacrylic acid group either directly at the macrocycle carbon (Type 1) or via macrocycle N-atom (Type 2), to unravel the structure-performance activity as solar dyes is investigated. These dyes were successfully adsorbed on noncrystalline TiO₂ particles, and efficient DSSCs have been constructed. The absorption and emission and electrochemical properties have been extensively studied and structures were modeled using DFT calculations. It was found that the Type 1 dyes cover wider spectral range compared to Type 2 dye. Similarly, Type 1 dyes were highly fluorescent compared to Type 2 dye, which was almost non-fluorescent. Electrochemical studies revealed harder oxidation potential for Type 1 dyes compared to Type 2 dyes, however, computational LUMO was found to be located mainly on cyanoacrylic acid group for both types of dyes, needed for efficient charge injection. The emission lifetime of the adsorbed dye was found to be drastically decreased upon surface adsorption suggesting occurrence of electron transfer (charge injection) from excited phenothiazine dye to TiO₂ conduction band.

The ability of both types of phenothiazine dyes to harvest light energy into electricity was evaluated by constructing two-electrode configuration sandwich type DSSCs. Both types of dyes were capable of producing significant amounts of photocurrent and photovoltage, however, Type 1 dyes superseded the Type 2 type dye in the present DSSC assembly. The frontier orbitals generated by MO calculation revealed location of the LUMOs to be appropriate for both types of dyes for electron injection from excited dye to TiO₂ conduction band. Interestingly, the oxidation potential for Type 2 dye is smaller than that of Type 1 dyes while the excited state energy of Type 2 dye is higher than that of Type 1 dye. This implies Type 2 dye to be better in terms of energetics of charge injection, however, lower performance of the solar device was observed. Two reasons could be attributed to the poor performance of Type 2 dye, viz., poor spectral coverage and lower emission quantum yields, and higher charge recombination resistance of Type 2 dye as evaluated from electrochemical impedance spectroscopy studies. The present studies demonstrate that the simple organic dyes based on phenothiazine reported here could serve as low cost alternate to ruthenium based expensive dyes, and their performance could be fine-tuned by appropriate macrocycle functionalization. Further studies, including broadening of absorption spectra and tuning energy levels, are in progress in our laboratory.

4. EXPERIMENTAL SECTION

Chemicals. All of the reagents were from Aldrich Chemicals (Milwaukee, WI) while the bulk solvents utilized in the syntheses were from Fischer Chemicals. Tetra-*n*-butylammonium perchlorate, (TBA)-ClO₄ used in electrochemical studies was from Fluka Chemicals.

Synthesis of Phenothiazine Derivatives. The general synthetic scheme and numbering of compounds is shown Scheme 1. Synthetic details are given below.

Tri(ethyleneglycol)monomethylether Tosylate (11). Tri(ethyleneglycol) monomethylether (3 ml, 19.14 mmol), dimethylaminopyridine (DMAP) (117 mg, 0.95 mmol), and triethyl amine (2.66 ml, 19.14 mmol) were dissolved in 100 mL of methylene chloride at 0 °C. To this mixture was added 20 mL of methylene chloride solution

of *p*-toluene sulfonyl chloride (3.65 g, 19.14 mmol) drop wise over a period of 20 min, and the whole mixture was stirred overnight at room temperature. The mixture was first treated with 200 mL of water and then 200 mL of saturated solution of sodium bicarbonate. The organic compound was extracted in methylene chloride and dried over Na₂SO₄. After evaporation of the solvent, the crude compound was purified by silica gel column. The desired compound was eluted with chloroform: methanol (95:5 v/v). Yield, 3.8 g (62.5%).

¹H NMR (400 MHz, CDCl₃): 2.38 ppm (s, 3H, -CH₃), 3.30 ppm (s, 3H, -CH₃), 3.45 ppm (t, 2H, -CH₂), 3.53 ppm (m, 6H, -CH₂), 3.62 ppm (t, 2H, -CH₂), 4.10 ppm (t, 2H, -CH₂), 7.23 ppm (d, 2H, Ar-H), 7.70 ppm (d, 2H, Ar-H). Mass-ESI: [M+H]⁺ obtained, 319.50; calcd, 318.30.

10-(2-hydroxyethane)phenothiazine (9). Compounds 8–10 were synthesized according to literature procedure with some modifications.^{44,45} To an ice-cooled suspension of NaH (60% in mineral oil, 600 mg, 25 mmol) in DMF (15 mL) was added phenothiazine (2 gm, 10.05 mmol) and 2-bromoethanol (0.71 ml, 10.05 mmol). The suspension was stirred at room temperature for 5 h under N₂. The mixture was cooled at room temperature and brine was added. The organic layer was collected with methylene chloride and dried over Na₂SO₄. After evaporation of solvent, the crude compound was purified over silica gel column and desired compound was eluted using hexane:CHCl₃ (50:50 v/v). Yield, 1.2 g (49 %).

¹H NMR (400 MHz: CDCl₃): 3.90 ppm (t, 2H, -CH₂), 4.10 ppm (t, 2H, -CH₂), 6.85 ppm (d, 2H, Ar-H), 6.95 ppm (t, 2H, Ar-H), 7.20 ppm (m, 4H, Ar-H). Mass-ESI: [M+H]⁺:obtained, 244.50; calcd, 243.60.

10-Triethyleneglycol Monomethylether Phenothiazine (10). To an ice-cooled suspension of NaH (60% in mineral oil, 600 mg, 25 mmol) in DMF (15 mL) was added phenothiazine (2 g, 10.05 mmol) and 11 (3.20 g, 10.05 mmol). The suspension was then stirred at room temperature for 5 h under N₂. The mixture was cooled at room temperature and brine was added. The organic layer was collected with methylene chloride and dried over Na₂SO₄. After evaporation of solvent, the crude compound was purified over silica gel column and desired compound was eluted by hexane: CHCl₃ (30:70 v/v). Yield, 1.3 g (38%).

¹H NMR (400 MHz:CDCl₃): 3.35 ppm (s, 3H, -CH₃), 3.35 ppm (m, 2H, -CH₂), 3.65 ppm (m, 6H, -CH₂), 3.85 ppm (t, 2H, -CH₂), 4.10 ppm (t, 2H, -CH₂), 6.90 ppm (m, 4H, Ar-H), 7.10 ppm (m, 4H, Ar-H). Mass-ESI: [M+H]⁺ obtained, 346.80; calcd, 345.50.

General Synthesis of Phenothiazine Carboxaldehyde Derivatives.

Compounds 1–7 were synthesized according to literature procedure with some modifications.^{46,47} A solution of phenothiazine derivative (N-methylphenothiazine (8, 9, or 10) in DMF (same amount that used for preparation of Vilsmeier complex) was added to the Vilsmeier complex (formed by mixing of POCl₃ and DMF at 0 °C and stirred for thirty minutes) and the mixture was heated overnight at 90 °C under N₂. All the constituents were used in the mole ratio of 1:1:7 of phenothiazine derivatives:POCl₃:DMF. After cooling at room temperature, the mixture was kept on ice bath and treated with saturated solution of NaOH till pH of the solution was reached slightly basic (pH 7–8); checked by litmus paper. Then the mixture was extracted in dichloromethane and dried over sodium sulfate and evaporated to get the crude compound, which was purified over silica gel column.

10-Methyl-3-formyl Phenothiazine (5). Eluted by hexane: CHCl₃ (80:20 v/v). Yield, 53%. ¹H NMR (400 MHz, CDCl₃): 3.40 ppm (s, 3H, -CH₃), 6.80 ppm (d, 2H, Ar-H), 6.95 ppm (t, 1H, Ar-H), 7.10 ppm (d, 1H, Ar-H), 7.20 ppm (t, 1H, Ar-H), 7.55 ppm (s, 1H, Ar-H), 7.65 ppm (d, 1H, Ar-H), 9.80 ppm (s, 1H, -CHO). Mass-ESI: [M+H]⁺ obtained, 242.60; calcd, 241.13.

10-(2-hydroxyethane)-3-formyl Phenothiazine (6). Eluted by hexane: CHCl₃ (60:40 v/v). Yield, 58.5%. ¹H NMR (400 MHz, CDCl₃): 3.80 ppm (t, 2H, -CH₂), 4.20 ppm (t, 2H, -CH₂), 6.90 ppm (m, 2H, Ar-H), 7.0 ppm (t, 1H, Ar-H), 7.15 ppm (m, 2H, Ar-H), 7.60 ppm (d, 1H, Ar-H), 7.65 ppm (d, 1H, Ar-H), 9.80 ppm (s, 1H, -CHO). Mass-ESI: [M+H]⁺ obtained, 272.40; calculated, 271.13.

10-Triethylene Monomethylether-3-formyl Phenothiazine (7). Eluted by hexane: CHCl₃ (20:80 v/v). Yield, 55.7%. ¹H NMR (400

MHz, CHCl_3): 3.40 ppm (s, 3H, CH_3), 3.50 ppm (m, 2H, $-\text{CH}_2$), 3.70 ppm (m, 6H, $-\text{CH}_2$), 3.85 ppm (t, 2H, $-\text{CH}_2$), 4.15 ppm (t, 2H, $-\text{CH}_2$), 6.90 ppm (m, 2H, Ar-H), 6.95 ppm (d, 1H, Ar-H), 7.15 ppm (m, 2H, Ar-H), 7.55 ppm (s, 1H, Ar-H), 7.65 ppm (dd, 1H, Ar-H), 9.80 ppm (s, 1H, $-\text{CHO}$). Mass-ESI: $[\text{M}+\text{H}]^+$ obtained, 374.40; calcd, 373.50.

10-(4-Formylphenyl) Phenothiazine (8). Phenothiazine (2 g, 10.05 mmol), 4-iodo benzaldehyde (2.33 g, 10.05 mmol), and CuO (3.59 g, 25.12 mmol) were kept in a 100 mL RB flask under N_2 and then heated at 160 °C with DMAc as a solvent for 18 h. After cooling at room temperature, the mixture was filtered. The filtrate was washed with water and extracted by with methylene chloride and dried over sodium sulfate. After evaporation of the solvent, the crude product was obtained, which was purified over a silica gel column. The desired compound was eluted by hexane: CHCl_3 (50:50 v/v). Yield, 1.5 g (49%). ^1H NMR (400 MHz, CDCl_3): 7.0 – 7.10 ppm (m, 4H, Ar-H), 7.15 – 7.25 ppm (m, 4H, Ar-H), 7.35 ppm (d, 2H, Ar-H), 7.65 ppm (d, 2H, Ar-H), 9.75 ppm (s, 1H, Ar-H). Mass-ESI: $[\text{M}+\text{H}]^+$ obtained, 305.30; calcd, 304.20.

Preparation of Phenothiazine Cyanoacrylic Acid Derivatives. Phenothiazine aldehyde derivatives and cyanoacetic acid (1:2 mol ratio) were mixed and refluxed in the presence of piperidine (catalytic amount) in acetonitrile (15 ml) as a solvent under N_2 for 5 h. After removing the solvent, mixture was washed with water and extracted by with methylene chloride and dried over Na_2SO_4 . After evaporation, the crude compound was obtained, which was purified by silica column. The desired compounds were eluted by CHCl_3 :MeOH (90:10 v/v).

10-Methyl-3-cyanoacrylic Acid Phenothiazine (1). Yield, 45%. ^1H NMR (400 MHz, CDCl_3): 3.40 ppm (s, 3H, $-\text{CH}_3$), 6.80 ppm (m, 2H, Ar-H), 6.95 ppm (t, 1H, Ar-H), 7.10 ppm (d, 1H, Ar-H), 7.20 ppm (t, 1H, Ar-H), 7.65 ppm (s, 1H, Ar-H), 7.80 ppm (d, 1H, Ar-H), 7.95 ppm (s, 1H, alkene-H). Mass-ESI: $[\text{M}]^+$ calcd, 308.35; found, 263.1, 277.1 (84%), 307.0 (80%) (100%). Elemental anal. Calcd for $\text{C}_{17}\text{H}_{12}\text{N}_2\text{O}_2\text{S}$: C, 66.21; H, 3.92; N, 9.08%. Found: C, 67.25; H, 4.69; N, 10.01%.

10-(2-Hydroxy ethane)-3-cyanoacrylic Acid Phenothiazine (2). Yield, 38%. ^1H NMR (400 MHz, CDCl_3): 3.60 ppm (t, 2H, $-\text{CH}_2$), 4.10 ppm (t, 2H, $-\text{CH}_2$), 6.65 ppm (d, 1H, Ar-H), 6.73 ppm (d, 1H, Ar-H), 6.93 ppm (t, 1H, Ar-H), 7.05 ppm (d, 1H, Ar-H), 7.15 ppm (t, 1H, Ar-H), 7.50 ppm (s, 1H, Ar-H), 7.70 ppm (d, 1H, Ar-H), 8.0 ppm (s, 1H, Alkene-H). Mass-ESI: $[\text{M}]^+$ calcd, 338.38; found, 326.2 (100%), 341.2 (10%). Elemental anal. Calcd for $\text{C}_{18}\text{H}_{14}\text{N}_2\text{O}_3\text{S}$: C, 63.89; H, 4.17; N, 8.28%. Found: C, 62.21; H, 4.65; N, 7.81%. FT-IR in KBr pallet (major peaks): 3412, 2949, 2213, 1620, 1593, 1571, 1468, 1360, 1334, 1221, 816, 751, 616 cm^{-1} .

10-Triethyleneglycol Monomethylether-3-cyanoacrylic Acid Phenothiazine (3). Yield, 30%. ^1H NMR (400 MHz, CDCl_3): 3.40 ppm (s, 3H, $-\text{CH}_3$), 3.60 ppm (t, 2H, $-\text{CH}_2$), 3.70 ppm (m, 6H, $-\text{CH}_2$), 3.90 ppm (t, 2H, $-\text{CH}_2$), 4.20 ppm (t, 2H, $-\text{CH}_2$), 6.65 ppm (d, 1H, Ar-H), 6.77 ppm (d, 1H, Ar-H), 6.93 ppm (t, 1H, Ar-H), 7.08 ppm (d, 1H, Ar-H), 7.15 ppm (t, 1H, Ar-H), 7.52 ppm (s, 1H, Ar-H), 7.65 ppm (d, 1H, Ar-H), 8.0 ppm (s, 1H, alkene-H). Mass-ESI: $[\text{M}]^+$ calcd, 440.50; found, 395.1 (100%), 439.1 (82%). Elemental anal. Calcd for $\text{C}_{23}\text{H}_{24}\text{N}_2\text{O}_3\text{S}$: C, 62.71; H, 5.41; N, 6.36%. Found: C, 60.57; H, 5.74; N, 6.82%. FT-IR in KBr pallet (major peaks): 3469, 2945, 3414, 2212, 1636, 1618, 1357, 1113, 812, 750, 617 cm^{-1} .

10-(4-Cyanoacrylic acid phenyl)phenothiazine (4). Yield, 30%. ^1H NMR (400 MHz, CDCl_3): 6.92 ppm (dd, 2H, Ar-H), 7.0 ppm (m, 2H, Ar-H), 7.10 ppm (m, 4H, Ar-H), 7.2 ppm (dd, 2H, Ar-H), 7.84 ppm (d, 2H, Ar-H), 8.0 ppm (s, 1H, alkene-H). Mass-ESI: $[\text{M}]^+$ calcd, 370.40; found, 325.1 (94%), 339.1 (92%), and 369.1 (100%). Elemental anal. Calcd for $\text{C}_{22}\text{H}_{14}\text{N}_2\text{O}_2\text{S}$: C, 71.33; H, 3.81; N, 7.56%. Found: C, 69.45; H, 5.09; N, 8.62%.

TiO₂ Electrode Preparation. FTO glass electrodes were first washed with soap and water, followed by sonication for 10 min in each of the following solutions: 0.1 M HCl in ethanol, bulk acetone, and bulk isopropanol. Following a drying period, the electrodes were then submerged in a 40 mM solution of TiCl_4 in Milli-Q water for 30 min at 75 °C. The electrodes were then washed with Milli-Q water, then MeOH before applying tape to each side, to control the film thickness

and provide space between the film and the edge of the FTO. Before applying the TiO_2 paste, each electrode was dusted thoroughly with nitrogen gas. The first layer applied used a paste derived from 20 nm TiO_2 particles (PST-18NR) using Doctor-blade technique and allowed to dry in air for twenty min. This was followed by a heating cycle at temperatures of 130, 230, 330, 395, 430, and 515 °C, for 10 min each. After allowing the electrode to cool at 80 °C, a second layer of 20 nm TiO_2 paste was then applied, followed by the same heating cycle. Lastly, a layer of 400 nm TiO_2 paste (PST-400C) was applied, followed by the heating cycle. After cooling, each piece of FTO was cut into 5–6 smaller electrodes of similar size. The electrodes were then submerged in a fresh 40 mM TiCl_4 solution for another 30 min at 75 °C. Afterwards, each electrode was submerged in a 0.3 mM dye solution in dichloromethane overnight with the TiO_2 film facing up.

Platinized Electrode Preparation. FTO glass electrodes were washed as stated above. After washing, each strip of FTO was heated at 440 °C for fifteen minutes, and then cooled at 80 °C for another 10 min. Each strip of FTO was then cut into 5–6 smaller electrodes of similar size. Each electrode was then dusted with N_2 before applying a solution containing 1 mg of chloroplatinic acid in 2 mL of EtOH. The electrodes were heated at 440 °C a second time, before allowing to cool.

Spectral Measurements. The UV–visible spectral measurements were carried out either on a Shimadzu Model 2550 double monochromator UV–visible spectrophotometer or a Jasco V-670 spectrophotometer. The steady-state fluorescence spectra were measured by using a Horiba Jobin Yvon Nanolog UV–visible-NIR spectrofluorometer equipped with a PMT (for UV–visible) and InGaAs (for NIR) detectors. The lifetimes were measured with the Time Correlated Single Photon Counting (TCSPC) lifetime option with nano-LED excitation sources on the Nanolog. The time calibration factor for system was 0.439 ns per channel. All the solutions were purged using nitrogen gas prior to spectral measurements. A right angle detection method was used for emission measurements. The ^1H NMR studies were carried out on a Varian 400 MHz spectrometer. Tetramethylsilane (TMS) was used as an internal standard. Differential pulse voltammograms were recorded on an EG&G 263A potentiostat/galvanostat using a three electrode system. A platinum button electrode was used as the working electrode. A platinum wire served as the counter electrode and an Ag/AgCl electrode was used as the reference electrode. Ferrocene/ferrocenium redox couple was used as an internal standard. All the solutions were purged prior to electrochemical and spectral measurements using argon gas. The computational calculations were performed by DFT B3LYP/6-31G* methods with GAUSSIAN 09 software package⁴² on high speed computers. The HOMO and LUMO orbitals were generated using *GuessView* program.

Photoelectrochemical and Electrochemical Impedance Measurements. Photoelectrochemical experiments were performed in a two-electrode configuration; thin films of TiO_2 on FTO was developed using Doctorblade technique according literature procedure.⁴ Photoelectrochemical cells were constructed using platinized ITO as counter electrode in acetonitrile containing a 0.5 M (*n*-Bu₄)NI and 0.03 M I₂ as redox mediator. The photocurrent–photovoltage characteristics of the solar cells were measured using a Model 2400 Current/Voltage Source Meter of Keithley Instruments, Inc. (Cleveland, OH) under illumination with an AM 1.5 simulated light source using a Model 9600 of 150 W Solar Simulator of Newport Corp. (Irvine, CA). Incident photon-to-current efficiency (IPCE) measurements were performed under ~4 mW cm^{-2} monochromatic light illumination conditions using a setup comprised of a 150 W Xe lamp with a Cornerstone 260 monochromator (Newport Corp., Irvine, CA).

Electrochemical impedance measurements were performed using EG&G PARSTAT 2273 potentiostat. Impedance data were recorded under forward bias condition from 100 kHz to 50 mHz with an A.C amplitude of 10 mV. Data were recorded under dark and A.M 1.5 illumination conditions applying corresponding open circuit potential (V_{oc}) for each electrode. The data were analyzed using ZSimpwin software from Princeton Applied Research. Solution resistance (R_s),

charge transfer resistance (R_{ct}), and capacitance due to constant phase element (Q) was deduced from the fitted data. CPE was considered as capacitance component of the double-layer electrode interface because of roughness of the electrode.

■ ASSOCIATED CONTENT

■ Supporting Information

Differential pulse voltammograms, fluorescence decay curves, solid-state absorption spectrum of FTO/TiO₂/dye electrodes, and ¹H NMR data of the newly synthesized compounds. This material is available free of charge via the Internet at <http://pubs.acs.org/>.

■ AUTHOR INFORMATION

■ Corresponding Author

*E-mail: Francis.DSouza@UNT.edu.

■ Notes

The authors declare no competing financial interest.

■ ACKNOWLEDGMENTS

This work was supported by the National Science Foundation (Grant 1110942 to FD).

■ REFERENCES

- O'Regan, B.; Grätzel, M. *Nature* **1991**, *353*, 737.
- Chen, S.; Xu, X.; Liu, Y.; Yu, G.; Sun, X.; Qiu, W.; Ma, Y.; Zhu, D. *Adv. Funct. Mater.* **2005**, *15*, 1541.
- Yoon, K. R.; Ko, S.-O.; Lee, S. M.; Lee, H. *Dyes Pigm.* **2007**, *75*, 567.
- Lai, R. Y.; Fabrizio, E. F.; Lu, L.; Jenekhe, S. A.; Bard, A. J. *J. Am. Chem. Soc.* **2001**, *123*, 9112.
- Tsai, Y.-L.; Chang, C.-C.; Kang, C.-C.; Chang, T.-C. *J. Lumin.* **2007**, *127*, 41.
- Roquet, S.; Cravino, A.; Leriche, P.; Alévêque, O.; Frère, P.; Roncali, J. *J. Am. Chem. Soc.* **2006**, *128*, 3459.
- Mishra, A.; Fischer, M. K. R.; Bäuerle, P. *Angew. Chem., Int. Ed.* **2009**, *48*, 2474.
- Hara, K.; Kurashige, M.; Ito, S.; Shinpo, A.; Suga, S.; Sayama, K.; Arakawa, H. *Chem. Commun.* **2003**, 252.
- Kitamura, T.; Ikeda, M.; Shigaki, K.; Inoue, T.; Anderson, N. A.; Ai, X.; Lian, T.; Yanagida, S. *Chem. Mater.* **2004**, *16*, 1806.
- Hara, K.; Sato, T.; Katoh, R.; Furube, A.; Yoshihara, T.; Murai, M.; Kurashige, M.; Ito, S.; Suga, S.; Arakawa, H. *Adv. Funct. Mater.* **2005**, *15*, 246.
- Wang, Z. S.; Cui, Y.; Dan-oh, Y.; Kasada, C.; Shinpo, A.; Hara, K. *J. Phys. Chem. C* **2007**, *111*, 7224.
- Xu, W.; Peng, B.; Chen, J.; Liang, M.; Cai, F. *J. Phys. Chem. C* **2008**, *112*, 874.
- Liu, W.-H.; Wu, I. C.; Lai, C.-H.; Lai, C.-H.; Chou, P.-T.; Li, Y.-T.; Chen, C.-L.; Hsu, Y.-Y.; Chi, Y. *Chem. Commun.* **2008**, 5152.
- Hwang, S.; Lee, J. H.; Park, C.; Lee, H.; Kim, C.; Park, C.; Lee, M.-H.; Lee, W.; Park, J.; Kim, K.; Park, N.-G.; Kim, C. *Chem. Commun.* **2007**, 4887.
- Ito, S.; Zakeeruddin, S. M.; Humphry-Baker, R.; Liska, P.; Charvet, R.; Comte, P.; Nazeeruddin, M. K.; Péchy, P.; Takata, M.; Miura, H.; Uchida, S.; Grätzel, M. *Adv. Mater.* **2006**, *18*, 1202.
- Ito, S.; Miura, H.; Uchida, S.; Takata, M.; Sumioka, K.; Liska, P.; Comte, P.; Péchy, P.; Grätzel, M. *Chem. Commun.* **2008**, 5194.
- Tian, H.; Yang, X.; Chen, R.; Pan, Y.; Li, L.; Hagfeldt, A.; Sun, L. *Chem. Commun.* **2007**, 3741.
- Cao, D.; Peng, J.; Hong, Y.; Fang, X.; Wang, L.; Meier, H. *Org. Lett.* **2011**, *13*, 1610.
- Xie, Z.; Midya, A.; Loh, K. P.; Adams, S.; Blackwood, D. J.; Wang, J.; Zhang, X.; Chen, Z. *Prog. Photovoltaics* **2010**, *18*, 573.
- Wu, W.; Yang, J.; Hua, J.; Tang, J.; Zhang, L.; Long, Y.; Tian, H. *J. Mater. Chem.* **2010**, *20*, 1772.
- Smestad, G. P.; Spiekermann, S.; Kowalik, J.; Grant, C. D.; Schwartzberg, A. D.; Adam, M.; Zhang, J.; Tolbert, L. M.; Moons, E. *Solar Energy Mater. Solar Cells* **2003**, *76*, 85–105.
- Wu, S.-L.; Lu, H.-P.; Yu, H.-T.; Chuang, S.-H.; Chiu, C.-L.; Lee, C. W.; Diau, E. W.-G.; Yeh, C.-Y. *Energy Environ. Sci.* **2010**, *3*, 949.
- (a) Lee, C. Y.; Hupp, J. T. *Langmuir* **2010**, *26*, 3760.
(b) Walter, M. G.; Rudine, A. B.; Wasmer, C. C. *J. Porphyrins Phthalocyanines* **2010**, *14*, 759.
- Kamat, P. V. *J. Phys. Chem. C* **2007**, *111*, 2834.
- (a) Umeyama, T.; Imahori, H. *Energy Environ. Sci.* **2008**, *1*, 120.
(b) Imahori, H.; Umeyama, T.; Kurotobi, K.; Takano, Y. *Chem. Commun.* **2012**, 48, 4032.
- Hasobe, T. *Phys. Chem. Chem. Phys.* **2010**, *12*, 44.
- Subbaiyan, N. K.; Wijesinghe, C. A.; D'Souza, F. *J. Am. Chem. Soc.* **2009**, *131*, 14646.
- Parussulo, A. L. A.; Iglesias, B. A.; Toma, H. E.; Araki, K. *Chem. Commun.* **2012**, 48, 6939.
- (a) Ragoussi, M.-E.; Cid, J.-J.; Yum, J.-H.; de la Torre, G.; Di Censo, D.; Grätzel, M.; Nazeeruddin, M. E.; Torres, T. *Angew. Chem. Int. Ed.* **2012**, *51*, 4375. (b) Martinez-Diaz, M. V.; de la Torre, G.; Torres, T. *Chem. Commun.* **2010**, 46, 7090.
- Sargent, E. H. *Nat. Photonics* **2012**, *6*, 133.
- Bang, J. H.; Kamat, P. V. *ACS Nano* **2009**, *3*, 1467.
- Tang, J.; Wang, X.; Brzozowski, L.; Barkhouse, D.; Aaron, R.; Debnath, R.; Levina, L.; Sargent, E. H. *Adv. Mater.* **2010**, *22*, 1398.
- D'Souza, F.; Ito, O. *Chem. Soc. Rev.* **2012**, *41*, 86.
- D'Souza, F.; Sandanayaka, A. S. D.; Ito, O. *J. Phys. Chem. Letts.* **2010**, *1*, 2586.
- Kamat, P. V.; Schatz, G. C. *J. Phys. Chem. C* **2009**, *113*, 15473.
- Rochford, J.; Chu, D.; Hagfeldt, A.; Galoppini, E. *J. Am. Chem. Soc.* **2007**, *129*, 4655.
- Wu, W.; Yang, J.; Hua, J.; Tang, J.; Zhang, L.; Long, Y.; Tian, H. *J. Mater. Chem.* **2010**, *20*, 1772.
- Wan, Z.; Jia, C.; Duan, Y.; Zhang, J.; Lin, Y.; Shi, Y. *Dye Pigm.* **2012**, *94*, 150.
- Xie, Z.; Midya, A.; Loh, K. P.; Adams, S.; Blackwood, D. J.; Wang, J.; Zhang, X.; Chen, Z. *Prog. Photovolt.: Res. Appl.* **2010**, *18*, 573.
- Marszalek, M.; Nagane, S.; Ichake, A.; Humphry-Baker, R.; Paul, V.; Zakeeruddin, S. M.; Grätzel, M. *J. Mater. Chem.* **2012**, *22*, 889.
- Hara, K.; Mori, S. S. *Handbook of Photovoltaic Science and Engineering*; Luque, A.; Hegedus, S., John Wiley: Chichester, U.K., 2011; p 642.
- Frisch, M. J.; Trucks, G. W.; Schlegel, H. B.; Scuseria, G. E.; Robb, M. A.; Cheeseman, J. R.; Zakrzewski, V. G.; Montgomery, J. A.; Stratmann, R. E.; Burant, J. C.; Dapprich, S.; Millam, J. M.; Daniels, A. D.; Kudin, K. N.; Strain, M. C.; Farkas, O.; Tomasi, J.; Barone, V.; Cossi, M.; Cammi, R.; Mennucci, B.; Pomelli, C.; Adamo, C.; Clifford, S.; Ochterski, J.; Petersson, G. A.; Ayala, P. Y.; Cui, Q.; Morokuma, K.; Malick, D. K.; Rabuck, A. D.; Raghavachari, K.; Foresman, J. B.; Cioslowski, J.; Ortiz, J. V.; Stefanov, B. B.; Liu, G.; Liashenko, A.; Piskorz, P.; Komaromi, I.; Gomperts, R.; Martin, R. L.; Fox, D. J.; Keith, T.; Al-Laham, M. A.; Peng, C. Y.; Nanayakkara, A.; Gonzalez, C.; Challacombe, M.; Gill, P. M. W.; Johnson, B. G.; Chen, W.; Wong, M. W.; Andres, J. L.; Head-Gordon, M.; Replogle, E. S.; Pople, J. A. *Gaussian 09*; Gaussian, Inc.: Pittsburgh, PA, 2009.
- Dye-Sensitized Solar Cells*; Kalyanasundaram, K., Ed.; EPFL Press: Lausanne, Switzerland, 2010.
- Xu, T.; Lu, R.; Liu, X.; Zheng, X.; Qui, X.; Zhao, Y. *Org. Lett.* **2007**, *9*, 797.
- Xu, T.; Lu, R.; Liu, X.; Chen, P.; Qui, X.; Zhao, Y. *Eur. J. Org. Chem.* **2008**, 1065.
- Tian, H.; Yang, X.; Chen, R.; Pan, Y.; Li, L.; Hagfeldt, A.; Sun, L. *Chem. Commun.* **2007**, 3741.
- Gaina, L.; Porumb, D.; Silaghi-Dumitrescu, I.; Cristea, C.; Silaghi-Dumitrescu, L. *Can. J. Chem.* **2010**, *88*, 42.